A model for enhanced fluid percolation in porous media by application of low-frequency elastic waves

Pavel P. Iassonov and Igor A. Beresnev

Department of Geological and Atmospheric Sciences, Iowa State University, Ames, Iowa, USA

Received 22 June 2001; revised 1 July 2002; accepted 12 December 2002; published 7 March 2003.

[1] Numerous observations and laboratory experiments suggest that elastic vibrations can significantly enhance transport of nonaqueous phase liquids (NAPLs) in porous media. Our analyses suggest that in the low-frequency range, capillary forces and nonlinear rheology of the fluid may be predominant mechanisms of vibratory stimulation. Consequently, a model of these mechanisms is built to explain the effect of sonic waves on fluid percolation. The model shows that the low-frequency elastic waves of relatively low intensity can significantly enhance the flow rate of a yield stress fluid under small external pressure gradients and aid in the mobilization of entrapped NAPL blobs by reducing the value of the threshold gradient needed to displace the fluid. We estimate the intensity of a sonic field to be used in the possible field implementation of this method to be in the range of $0.2-125$ W/m^2. *INDEX TERMS:* 1832 Hydrology: Groundwater transport; 0935 Exploration Geophysics: Seismic methods (3025); 5139 Physical Properties of Rocks: Transport properties; *KEYWORDS:* vibrations, sonic stimulation, enhanced fluid flow, NAPL, non-Newtonian fluid, capillary trapping

Citation: Iassonov, P. P., and I. A. Beresnev, A model for enhanced fluid percolation in porous media by application of low-frequency elastic waves, *J. Geophys. Res.*, *108*(B3), 2138, doi:10.1029/2001JB000683, 2003.

1. Introduction

[2] The subject of vibratory (sonic or seismic) stimulation of fluid flow in porous media has aroused increasing interest in the last decade, primarily in connection with the applications to enhanced oil recovery (EOR) and remediation of nonaqueous phase liquids (NAPL) contaminated aquifers. Compared to the other methods of EOR currently in use, the vibratory stimulation is ecologically clean and economic in its implementation, which promotes its further use.

[3] There are numerous laboratory experiments and field observations (see *Beresnev and Johnson* [1994] for a review of existing publications) that provide evidence that sonic stimulation can significantly enhance fluid flow in porous media. Documented observations include such effects as changes in water level in wells, and, more importantly, oil production changes in response to various seismic sources. Most of these observations, however, are of little use in quantitative analyses due to the scarcity of data and the complexity of the phenomena involved. For example, the effects of an earthquake on an oil reservoir might have been caused not only by elastic vibrations, but also by fracturing, subsidence, or compression of surrounding rocks. The data reported are also often inconsistent and contradictory [*Beresnev and Johnson*, 1994].

[4] In the following years, numerous laboratory studies, prompted by the field observations and the potential benefits of the method shed more light on the problem, providing more detailed observations of the elastic wave effect on percolation through porous media. The frequency-dependant increase in the rate of oil displacement, decrease in oil viscosity, coalescence of oil droplets, acceleration in gravity-driven draining of porous samples are just a few of the phenomena observed under laboratory conditions [*Beresnev and Johnson*, 1994].

[5] The problem that the method currently faces, though, is that the physical mechanisms by which the elastic waves mobilize porous fluids are largely unclear [*Beresnev and Johnson*, 1994; *Drake and Beresnev*, 1999; *Roberts et al.*, 2001], and there is no reliable model that could predict the effect of stimulation or help design an optimum field setup.

[6] There are several mechanisms thought to be responsible for the observed effects of sound on fluid percolation in porous media [*Aarts and Ooms*, 1998; *Beresnev and Johnson*, 1994; *Drake and Beresnev*, 1999; *Nikolaevskiy et al.*, 1996; *Roberts et al.*, 2001], operating in different frequency ranges. The effect of high-frequency waves is limited to very short distances from the source, due to high sound absorption, and will not be considered here. On the other hand, based on published evidence and existing theoretical work, one may conclude that, in the lower-frequency range, the important mechanisms governing flow enhancement are nonlinear fluid rheology and capillary effects.

[7] Another possible mechanism that can play role in flow stimulation in the low-frequency range is the poroelastic motion, which reflects volumetric changes in pores in response to stress and pore pressure, due to the elasticity of the solid [*Wang*, 2000]. It is invoked in the studies of high-pressure pulse treatment of reservoirs, a known method of EOR [*Spanos et al.*, 1999], whose mechanisms, however, are different from the weak elastic wave stimulation. The

Copyright 2003 by the American Geophysical Union.
0148-0227/03/2001JB000683$09.00

effect of elastic vibrations on fluid flow in a porous medium composed of elastic channel structures has been addressed by *Pan and Horne* [2000] and shown to produce a relatively little flow enhancement, and only at resonant frequencies, which strongly depend on the porosity of the medium. Because of natural variations in porosity and limited variability in the frequency of operation of available seismic sources [*Drake and Beresnev*, 1999], this resonant method appears to be of little applicability to realistic reservoir conditions. Thus we do not consider poroelastic effects, and focus on non-Newtonian rheology and capillary trapping in relation to vibration-induced relative motion of fluid and solid.

[8] Numerous theoretical and experimental investigations have demonstrated that vibration can have a significant effect on the flow of non-Newtonian fluids in general [*Kazakia and Rivlin*, 1978; *Mena et al.*, 1979; *Goshawk and Waters*, 1994; *Rahaman and Ramkissoon*, 1995; *del Rio et al.*, 1998; *Tsiklauri and Beresnev*, 2001a, 2001b]. The most important result of the aforementioned studies is that, for various rheological models, the flow of a non-Newtonian fluid can be significantly enhanced by application of vibrations parallel to the main flow. The significance of capillary forces in multiphase flow is well known as well [*Bear*, 1988; *Hilpert et al.*, 2000]. The contribution of both of these mechanisms is theoretically investigated below. We provide a simple theoretical model that could be used for practical calculations of the effect of vibrations on the flow based on the rheology of realistic nonaqueous fluids and the physics of capillary phenomena.

2. Yield Stress Model

2.1. Constitutive Relationship

[9] Oil is typically considered a Newtonian fluid. It has been demonstrated, though, that under reservoir conditions it often exhibits nonlinear behavior (due to interaction with the solid matrix and the properties of high-polymer constituent components [*Bird et al.*, 1987]) that can be described using a threshold gradient filtration model [*Nikolaevskiy*, 1996]. The latter approximates the yield stress (Bingham plastic) fluid behavior [*Papanastasiou*, 1987]. For oils with significant content of high-polymer components (e.g., waxy crude oil), the existence of significant yield stress rheology has been verified in laboratory experiments [*Wardhaugh and Boger*, 1991].

[10] The constitutive law relating the stress and the strain rate of a yield stress fluid in one-dimensional case (schematically illustrated in Figure 1) can be written as

$$\begin{aligned} \dot{\gamma} &= 0 && |\tau| < \tau_0 \\ \tau &= \left(\mu + \frac{\tau_0}{|\dot{\gamma}|}\right)\dot{\gamma} && |\tau| \geq \tau_0 \end{aligned}, \tag{1}$$

where τ, $\dot{\gamma}$, τ_0, and μ are the stress, strain rate, yield stress, and dynamic viscosity, respectively. This law physically means that the fluid starts to flow when a certain threshold stress (yield stress τ_0) is applied.

2.2. Governing Equations

[11] In this section, we present a simple model that can be used to estimate the effect of low-frequency sound on the flow of Bingham (yield stress) fluid in a straight tube of circular cross section and constant radius. The effect of sonic wave is represented as longitudinal vibrations (with given frequency and amplitude) of the tube. The fluid is assumed incompressible, and the effects of gravity are neglected.

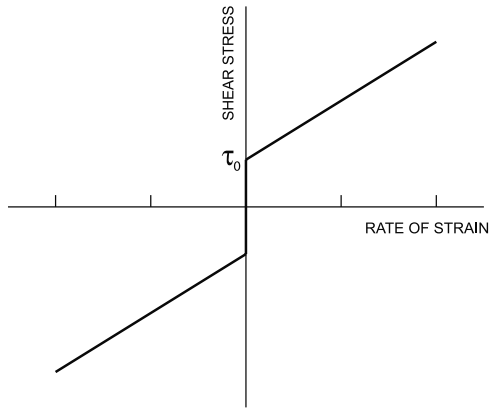

Figure 1. The stress as a function of the rate of strain for the Bingham fluid model.

[12] The governing equation in this case is the momentum equation [*Schetz and Fuhs*, 1999],

$$\rho\frac{\partial \boldsymbol{v}}{\partial t} + \rho(\boldsymbol{v}\cdot\nabla)\boldsymbol{v} = -\nabla p + \nabla\cdot\boldsymbol{\tau}. \tag{2}$$

Here $\boldsymbol{v}$, p, and ρ denote the particle velocity vector, pressure, and density of the fluid, respectively, and $\boldsymbol{\tau}$ represents the stress tensor.

[13] We assume that the flow is axisymmetric and that the wall vibration phase changes slowly along the tube, thus allowing us to neglect the changes in fluid velocity along the axis of the tube as well. The latter assumption is reasonable in the low-frequency range (below 100 Hz) of interest in this paper, in which the wavelengths in a typical oil-bearing rock are on the order of tens to hundreds of meters. Under these assumptions, the pressure gradient and the velocity components normal to the wall of the tube can be neglected, and the contribution of the nonlinear term in equation (2) becomes negligibly small. Thus, in the cylindrical coordinate system, equation (2) becomes

$$\rho\frac{\partial v}{\partial t} = \left(-\frac{\partial p}{\partial z}\right) + \frac{1}{r}\frac{\partial}{\partial r}(r\tau), \tag{3}$$

where v is the z component of fluid velocity (oriented along the axis of the tube), and $\tau = \tau_{rz}$. Relationship (1) between stress and strain rate can be written in terms of fluid velocity [*Schetz and Fuhs*, 1999] as

$$\begin{aligned} \mu\frac{\partial v}{\partial r} &= 0 && \tau < \tau_0 \\ \mu\frac{\partial v}{\partial r} &= \tau - \tau_0 && \tau \geq \tau_0 \end{aligned}. \tag{4}$$

2.3. Steady State Flow

[14] The steady state (time-independent) analog of equation (3) is

$$\frac{\partial p}{\partial z} = \frac{1}{r}\frac{\partial}{\partial r}(r\tau). \tag{5}$$

In the following, we use a no-slip boundary condition (the wall is immobile in the steady state case)

$$v(R) = 0, \tag{6}$$

where R is the radius of the tube, and assume an external constant pressure gradient G,

$$\frac{\partial p}{\partial z} = G. \tag{7}$$

[15] Solving equation (5) for τ, we obtain

$$\tau = G\frac{r}{2}. \tag{8}$$

The solution for the velocity v will consist of two parts, depending on the value of shear stress with respect to τ_0 according to rheology equation (4). From the solution (8), we can see that the condition $\tau < \tau_0$ is equivalent to $r < r_0$, where

$$r_0 = 2\tau_0/G. \tag{9}$$

The parameter r_0 defines the radius of the inner part of the cylindrical flow where shear stress is below the value of yield stress, and, according to equation (4), the fluid moves as a "solid" cylinder with constant velocity. Considering the boundary condition (6), we can see that, for r_0 larger than the radius of the tube R, the only solution of equation (5) is $v(r) = 0$. Thus, for any given pressure gradient, the flow will only occur in pore channels with radii $R > r_0$. If r_0 does not exceed R, however, the solution of equation (5) is

$$\begin{aligned} v(r) &= -\frac{R^2}{4\mu}\left(1-\frac{r_0}{R}\right)^2 G = \text{const} \qquad r < r_0 \\ v(r) &= \frac{1}{\mu}\left[\frac{1}{4}\left(r^2-R^2\right)G - (r-R)\tau_0\right] \quad r \geq r_0 \end{aligned}. \tag{10}$$

[16] The net flow rate through the tube can then be calculated as

$$Q = 2\pi\int_0^R v(r) r dr. \tag{11}$$

The integration yields

$$\begin{aligned} Q &= -\frac{\pi R^4}{8\mu}\left(1-\frac{4}{3}\xi+2\xi^2-4\xi^3+\frac{7}{3}\xi^4\right)G \quad \xi < 1 \\ Q &= 0 \qquad\qquad\qquad\qquad\qquad\qquad\quad \xi \geq 1 \end{aligned}, \tag{12}$$

where

$$\xi = \frac{r_0}{R}. \tag{13}$$

[17] Using equations (13) and (9), the condition $\xi < 1$ from equation (12) can be rewritten as $G > G_{\text{crit}}$, where

$$G_{\text{crit}} = 2\tau_0/R. \tag{14}$$

The latter defines the minimal external pressure gradient required to mobilize the yield stress fluid in a pore channel of a given radius.

2.4. Flow Under Effect of Vibration

[18] We model the effect of sonic wave as longitudinal vibrations of the channel wall parallel to the tube axis, with the given amplitude and frequency. The displacement of the wall is

$$w = ae^{i\omega\cdot t}, \tag{15}$$

where a is the displacement amplitude and ω is the angular frequency of vibration.

[19] Introducing the relative velocity of the fluid with respect to the wall,

$$U = (v - \dot{w}), \tag{16}$$

we can rewrite equation (3) as

$$\rho\frac{\partial U}{\partial t} = X + \frac{1}{r}\frac{\partial}{\partial r}(r\tau), \tag{17}$$

where

$$X = \rho\frac{\partial^2 w}{\partial t^2} - \frac{\partial p}{\partial z} = -\rho a\omega^2 e^{i\omega t} - \frac{\partial p}{\partial z}, \tag{18}$$

which can be considered an external volume force. It is, effectively, the inertial force acting on the fluid because of the pore wall (solid skeleton) oscillations. This term, along with the no-slip boundary condition, is what determines the coupling between the fluid and the solid matrix in our model when vibrations are present.

[20] The no-slip boundary condition becomes

$$U(R) = 0. \tag{19}$$

[21] For frequencies below a certain "critical" value,

$$f_c = \frac{\pi\mu}{4\rho d^2}, \tag{20}$$

where d is the average diameter of the pores, the flow of a Newtonian fluid in a pore channel can be considered quasi-steady [*Biot*, 1956]. Although this condition was obtained for a Newtonian fluid, it will also hold for the yield stress fluid with the same value of dynamic viscosity [*Papanastasiou*, 1987]. For a typical oil reservoir pore diameter of 0.1 mm, density and viscosity

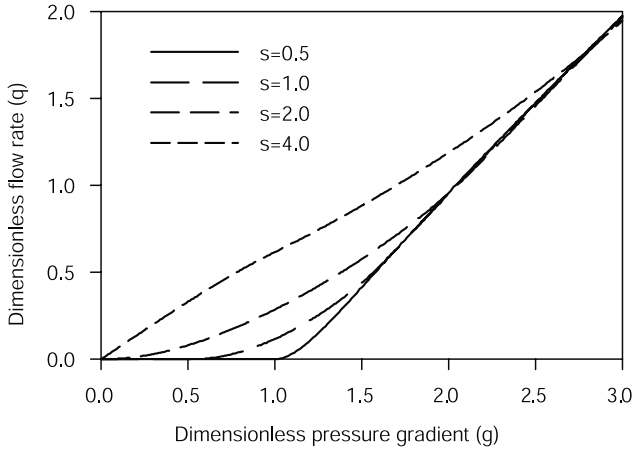

Figure 2. Dimensionless flow rate q versus dimensionless pressure gradient g (defined in text) for various values of the effective amplitude of vibration s (dimensionless).

of crude oil of 800 kg/m^3 and 5 mPa s, respectively, we obtain $f_c \approx 500$ Hz.

[22] Since we are interested in the low-frequency range effects only (frequencies of the order of 100 Hz and less, which is well below the critical frequency (equation (20))), the time derivative in equation (17) can be neglected [*Biot*, 1956]. Under this assumption, equation (17) becomes identical to equation (5) except that the pressure gradient term is replaced with the external volume force (equation (18)). The solution will thus still be provided by equation (12). The only difference is that X includes an oscillatory term, so we need to calculate the time average to obtain the net flow rate:

$$\langle Q \rangle = \frac{1}{T} \int_0^T Q(t)dt, \tag{21}$$

where T is the period of oscillations.

[23] Since the effect of vibration in our model is equivalent to the addition of an oscillating term to the pressure gradient (compare equations (3) and (17)–(18)), it will effectively increase the flow rate when the vibration-induced volume force (equation (18)) is acting in the same direction as the external pressure gradient, and decrease it in the opposite phase of the wave. Consequently, even though the average of the vibration-induced volume force term in equation (18) over an oscillation period is zero, its net effect on the flow rate (equation (21)) will not average out to zero for nonzero pressure gradients due to nonlinearity in equation (12) (considering that ξ in equation (12) includes the pressure gradient term (equations (9) and (13)), which, for the case of applied vibration, contains the external field (equation (18)).

[24] The results presented in later sections are obtained by numerical integration of equation (21) using solution (12). Since a high number of data points could be generated, the simple trapezoidal rule was used for integration, with the resulting relative precision of 10^{-9}.

2.5. Results

[25] It is convenient to analyze the solution in terms of the following dimensionless variables, representing the flow rate, pressure gradient, and amplitude of oscillations, respectively:

$$q = Q/Q_P(G_{\text{crit}}),$$

$$g = G/G_{\text{crit}}, \tag{22}$$

$$s = \rho a \omega^2 / G_{\text{crit}},$$

where Q is defined by equation (21), and Q_P (G) is the Poiseuille flow rate (the flow rate of a Newtonian fluid in the same tube [*Schetz and Fuhs*, 1999]),

$$Q_P(G) = -\frac{\pi R^4}{8\mu} G. \tag{23}$$

[26] Figure 2 presents the dependence of the dimensionless flow rate q on the external pressure gradient g for several values of the amplitude of vibration s. Figure 3, conversely, demonstrates the dependence of q on s for different values of g. From Figure 2, the most noticable effect of vibration is the decrease in the critical pressure gradient below which no flow occurs, for a given pore diameter. For a real porous medium, this would mean mobilization of fluid otherwise stagnant (trapped) in the pores of small size (equations (12) and (13)), therefore decreasing the amount of residual oil in the reservoir. Figure 3 shows that the sound also increases the flow rate for a given pressure gradient.

[27] Figure 4 demonstrates the relative increase in the flow rate due to vibrations,

$$J(q_0) = \frac{q - q_0}{q_0}, \tag{24}$$

where q_0 denotes the steady state flow rate (no vibrations applied). It can be observed that, for the low values of q_0, the relative increase in the flow rate can be very high, while for the higher values of q_0, the relative increase is much smaller. Note that the values of J at near-zero values of q_0 are of no practical importance, since they correspond to

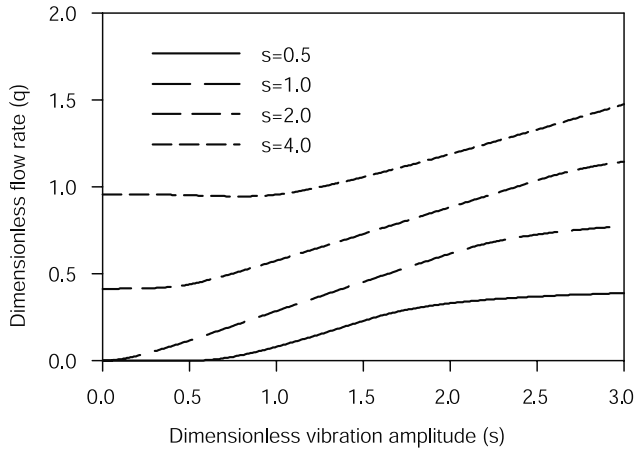

Figure 3. Dimensionless flow rate q versus effective vibration amplitude s (defined in text), for various values of the dimensionless pressure gradient g.

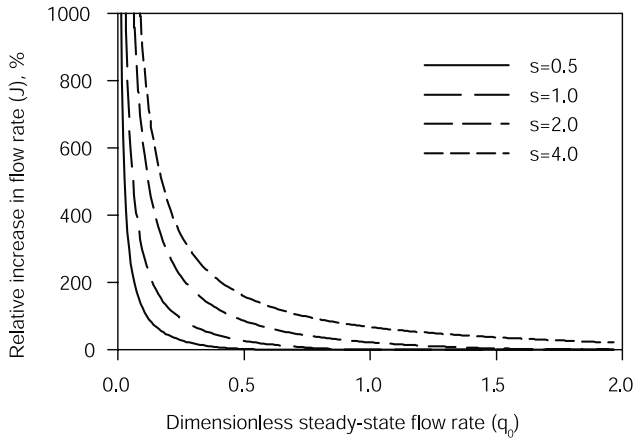

Figure 4. Relative increase in flow rate due to vibrations versus steady state flow rate (no vibrations applied) for various values of the effective amplitude of vibration s.

near-zero external pressure gradients (negligibly small flow rates). In other words, vibrations cannot induce the flow of fluid at rest in this model, they can only aid in further mobilization of the fluid already in motion; this explains J tending to infinity as q_0 tends to zero.

2.6. Estimation of Stimulation Parameters

[28] To estimate the parameters of a sonic field required to achieve a significant effect in mobilization of the entrapped fluid, we need to know the value of the yield stress τ_0. The general problem with the values of this quantity in oil under reservoir conditions is that there are no reliable data on it. Apparently, the values of yield stress are typically too small and are of no direct interest to most exploration or production applications; this may explain why insufficient attention has been paid to its accurate measurements. The exception is crude waxy oil, where nonlinear rheology is more pronounced and is of practical significance due to applications in pipeline transportation [*Chang et al.*, 1999]. Thus the values for yield stress we use in this study are estimates only.

[29] The yield stress parameter can vary significantly depending on oil composition, temperature and the dynamics of the sharing process from near-zero values (for high-grade oil components) to the values on the order of 1 Pa for waxy crude oils at low temperatures [*Wardhaugh and Boger*, 1991]. Under reservoir conditions, however (due to high temperatures), we should expect much lower values of yield stress [*Wardhaugh and Boger*, 1991]. We estimate the typical values of τ_0 to be in the range of 0.002–0.05 Pa, which, for R = 0.05 mm, will result in the values of critical pressure gradient (equation (14)) of 80–2000 Pa/m.

[30] It is common to use the intensity of a continuous monochromatic sonic wave [*Telford et al.*, 1996, equation 4.30] to characterize the physical effects of vibrations,

$$I = \frac{1}{2} a^2 \omega^2 V \rho_p, \tag{25}$$

where V and ρ_p are the sound velocity and average density of the saturated porous medium.

[31] To estimate the intensity needed to mobilize the fluid, we note that the flow of the yield stress fluid will only start when

$$\max|X| > G_{\text{crit}}. \tag{26}$$

[32] For infinitesimally small pressure gradients, we rewrite equation (26) using equation (18) as

$$\rho a \omega^2 > G_{\text{crit}}. \tag{27}$$

Substituting the value of the amplitude of vibrations a obtained from equation (27) into equation (25), we obtain

$$I_c = \frac{\rho_p V}{2\omega^2 \rho^2} G_{\text{crit}}^2. \tag{28}$$

Equation (28) gives an exact value for the case of vibrations along the pore tube's axis. For an arbitrarily oriented channel, it will include a coefficient defined by the angle between the channel's axis and the direction of the displacement in the wave. There can be additional macroscopic parameters controlling the applicability of this analysis to the real porous media, such as direction of propagation and type of elastic wave (compressional or shear) in relation to the flow direction and preferred pore orientation. In the latter calculations, we assume a compressional wave propagating along the flow direction, which is defined by the external pressure gradient. The qualitative inferences of the analysis will not change if another wave type is considered.

[33] Using the parameters typical of oil-bearing sandstones, V = 2000 m/s, ρ_p = 2000 kg/m^3, ρ = 800 kg/m^3 (density of oil), and the frequency of 100 Hz, for the range of critical pressure gradient listed above, we obtain I_c in the range of 0.2–125 W/m^2. For the porous media with larger pore size, the critical pressure gradient will be lower (equation (14)), and therefore the minimal required intensity I_c (equation (28)) will be smaller too. Increasing the frequency will also decrease I_c. It should be remembered, though, that an increase in frequency will also result in higher wave attenuation, and, therefore, it will be more difficult to deliver the intensity I_c, required to mobilize the fluid, to a particular part of geologic formation.

2.7. Flow in Two-Fluid System

[34] Let us define the efficiency of oil recovery as the percentage of oil in the total produced fluid. To estimate the effect of vibrations on this parameter, we consider a model of porous medium saturated by two immiscible fluids, occupying separate (nonmixing) volumes of the reservoir (Figure 5), one of which (oil) exhibits the yield stress behavior, while the other (water) is a Newtonian fluid. We will assume 100% saturation of both fluids in their respec-

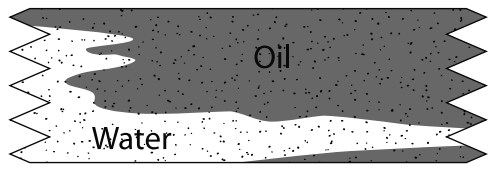

Figure 5. Representation of reservoir used in the model of a two-fluid system.

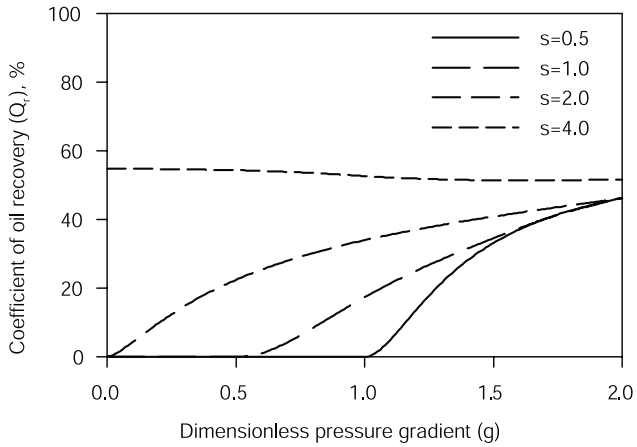

Figure 6. Coefficient of oil recovery, defined in the text, versus dimensionless pressure gradient g (fraction of volume of the reservoir occupied by water α = 10%), for various values of the effective amplitude of vibration s.

tive domains and the same external pressure gradient G acting on both oil and water. The longitudinal vibrations of the pore walls will not change the net flow rate of a Newtonian fluid [*Kazakia and Rivlin*, 1978]; thus we can write equation (23) as

$$Q_w(G) = -\frac{\pi R^4}{8\mu_w} G, \tag{29}$$

where μ_w is the viscosity of water. The flow rate of oil (Q_{oil}) can be calculated as before using equations (12)–(14), (18), and (21). The fraction of the volume of oil flowing through a unit area of reservoir to the total volume of fluid, which is the coefficient of recovery, is then

$$Q_r = \frac{(1-\alpha)Q_{\text{oil}}}{\alpha Q_w + (1-\alpha)Q_{\text{oil}}}, \tag{30}$$

where α is the fraction of volume of the reservoir occupied by water. Figure 6 shows Q_r as a function of pressure gradient in the same dimensionless units as above. Viscosity of water μ_w was taken to be five times smaller than that of oil; water was assumed to occupy 10% of the pores (α = 0.1). Figure 6 demonstrates that the application of sonic vibrations significantly increases the outflowing oil-to-water ratio, especially for the relatively low values of pressure gradient, allowing higher efficiency of oil recovery under the same pressure field conditions.

3. Capillary Forces

3.1. The Problem

[35] The effect of capillary forces on fluid percolation through a pore channel can be viewed as equivalent to that of finite yield stress in the fluid, in that the flow can only begin when a certain threshold pressure gradient is applied. This equivalence occurs due to the phenomenon of capillary trapping, which takes place when the meniscus is "pinned" on mechanical irregularities or chemical impurities on the walls, so that a finite force is needed to release the contact line [*de Gennes*, 1985; *Leger and Joanny*, 1992; *Hilpert et al.*, 2000].

[36] For the purposes of this analysis, we assume oil to be a Newtonian fluid (to avoid unnecessary complications of the model, since our goal is to estimate the effect of capillary trapping independent of other mechanisms). The geometry of the problem is modeled as that of an oil blob trapped in a pore channel of circular cross section (the length of the blob is much larger than the radius of the channel), confined from both sides by the spherical water-oil interfaces (Figure 7a). Pore walls vibrate longitudinally with the given frequency and amplitude.

[37] To model the capillary pinning of the menisci, we assume that the surface of the wall is sufficiently rough, to be able to "trap" the three-phase contact line. The roughness heights are assumed to be small enough not to noticeably affect the flow in the tube.

3.2. Governing Equations and Solution

[38] The governing equation for this problem is the same as equation (2), except τ represents the Newtonian viscous stress tensor. Since $L \gg R$, the velocity field in the blob may be approximated by that in an infinitely long tube. In this case, the governing equation for this problem becomes identical to equation (3), except that τ represents pure viscous stress, which for axisymmetric flow of Newtonian fluid is

$$\tau = \mu \frac{\partial v}{\partial r}, \tag{31}$$

where μ denotes the dynamic viscosity of oil, and v, as before, is the z component of fluid velocity. Substituting equation (31) into equation (3) and introducing the relative velocity U (equation (16)), we write

$$\rho \frac{\partial U}{\partial t} = X + \frac{1}{r}\frac{\partial}{\partial r}\left(r\mu \frac{\partial U}{\partial r}\right), \tag{32}$$

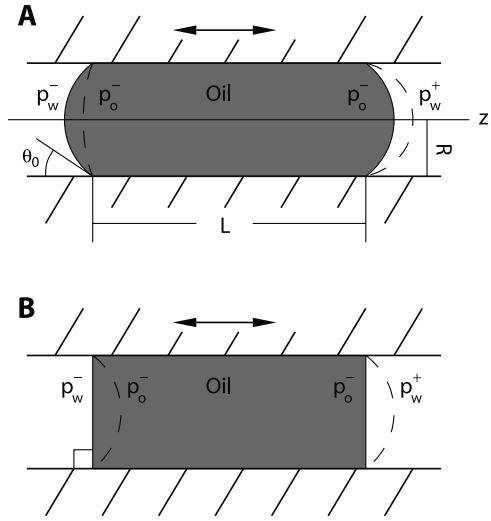

Figure 7. Geometry of a capillary-trapped oil blob with pinned contact lines in a cylindrical pore channel. Solid lines indicate equilibrium state with no external pressure gradient; dashed lines indicate external pressure gradient applied. (a) General case; (b) equilibrium contact angle 90°.

where X is defined by equation (18). Assuming quasi-static conditions (see section 2.4), we write the solution of equation (32) as

$$U(r,t) = \frac{1}{4\mu}\left(r^2 - R^2\right)X(t). \tag{33}$$

Knowing the velocity profile, we can calculate the flow rate (equation (11)):

$$Q(t) = \frac{\pi R^4}{8\mu}X(t). \tag{34}$$

3.3. Capillary Parameters and Pressure Balance

[39] The constant pressure gradient part of X (equation (18)) can be calculated as

$$\frac{\partial p}{\partial z} = \frac{\Delta p_o}{L}, \tag{35}$$

where $\Delta p_o = p_o^+ - p_o^-$ is the pressure difference between both menisci in oil (hereafter the superscript pluses and minuses refer to the right (larger z) and left (smaller z) menisci, respectively) (Figure 7a). Neglecting the effect of gravity, Δp_o can be calculated using the pressure balance equations on each meniscus,

$$p_o^{\pm} = p_w^{\pm} + p_c^{\pm}, \tag{36}$$

where $p_w^{\pm}$ define the pressure in water on each side of the blob, and $p_c^{\pm}$ are the capillary pressures.

[40] While the values $p_w^{\pm}$ are unknown, the pressure difference in water between both menisci can be approximated using the known value of the external pressure gradient G that acts on both oil and surrounding water (this approximation is possible due to the assumption that the existence of oil blob does not significantly affect the macroscopic flow of water in the regions surrounding the blob),

$$p_w^+ - p_w^- = G \cdot L. \tag{37}$$

Substituting equations (36) and (37) into equation (35), we obtain

$$\frac{\partial p}{\partial z} = G + \frac{p_c^+ - p_c^-}{L}. \tag{38}$$

[41] The behavior of $p_c^{\pm}$ depends on the equilibrium (no external pressure gradient, no vibration) state of each meniscus, defined by the contact angles $\theta_0^{\pm}$. In natural systems, one can expect this parameter to vary over a wide range (due to different material properties and complex geometry), which makes it difficult to use equation (38) directly.

[42] For the purposes of our analysis, we approximate equation (38) by assuming the equilibrium contact angles $\theta_0^{\pm} = 90°$. This choice of the contact angle is made as an approximation allowing a simple use of the obtained formulae to provide an estimate of the effect of vibration. Precise treatment of this problem would not only require the knowledge of the actual contact angles, but also consideration of the fact that, generally, each meniscus would reach the critical pressure independently, at different times, resulting in unsteady flow regimes and other complicated phenomena; these were not possible to address in this article.

[43] In case of the equilibrium contact angle $\theta_0^{\pm} = 90°$, the two menisci at any given time will have the same modulus but a different sign of the radius of curvature, as illustrated in Figure 7b. Considering equation (36), this assumption yields

$$p_c^+ = -p_c^- = p_c. \tag{39}$$

Equation (34) then becomes

$$Q = \frac{\pi R^4}{8\mu}\left(X^* - \frac{2p_c}{L}\right), \tag{40}$$

where

$$X^* = -\rho a \omega^2 e^{j\omega t} - G. \tag{41}$$

[44] For the capillary pressure p_c smaller than some critical value $(p_c)_{\text{crit}}$, the three-phase contact line will remain pinned [*de Gennes*, 1985; *Charlaix and Gayvallet*, 1992; *Leger and Joanny*, 1992], and therefore no flow will occur. If the capillary pressure exceeds the critical value (which is equivalent to some finite force needed to mobilize the menisci), the blob will become mobile. However, as soon as the capillary pressure on the menisci drops below $(p_c)_{\text{crit}}$, the flow will stop again. This process can thus be described as the flow with a critical pressure gradient, which is dependent on $(p_c)_{\text{crit}}$. Given that, we can rewrite equation (40) in the form

$$\begin{array}{ll} Q(t) = \dfrac{\pi R^4}{8\mu}(X^* - C) & |X^*| \geq C \\ Q(t) = 0 & |X^*| < C \end{array}, \tag{42}$$

where C denotes the minimum pressure gradient required to mobilize a particular oil blob,

$$C = 2(p_c)_{\text{crit}}/L. \tag{43}$$

The net flow rate can be calculated using equation (21) as before.

3.4. Results

[45] The critical capillary pressure $(p_c)_{\text{crit}}$ can vary significantly, depending on local geometry of the pores, roughness and chemical composition of the pore walls, etc. [*de Gennes*, 1985]. We can, however, estimate the upper bound for this parameter from the Laplace's capillary equation using the pore radius R (which is the minimum possible radius of curvature of a spherical meniscus in a cylindrical tube):

$$(p_c)_{\text{crit}} \leq 2\sigma/R, \tag{44}$$

where σ is the surface tension. The typical value for $(p_c)_{\text{crit}}$ will be significantly less, probably on the order of half of the top estimate equation (44) [*Charlaix and Gayvallet*, 1992].

[46] As an example, we consider an oil blob in a medium with an average pore radius of 0.05 mm. For $\sigma = 20$ mN/m

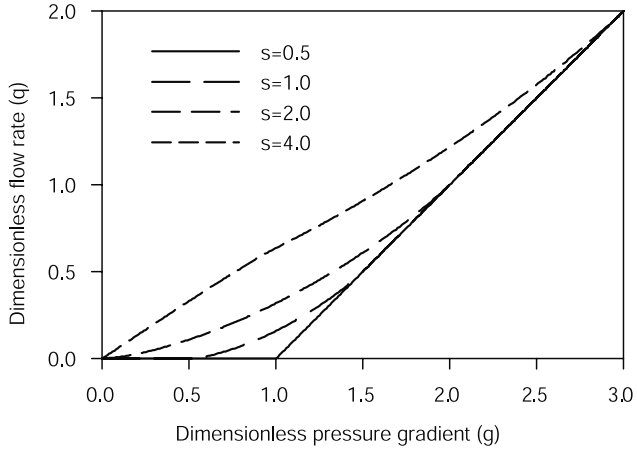

Figure 8. Dimensionless flow rate q of a capillary blob versus dimensionless pressure gradient g for various values of the effective amplitude of vibration s.

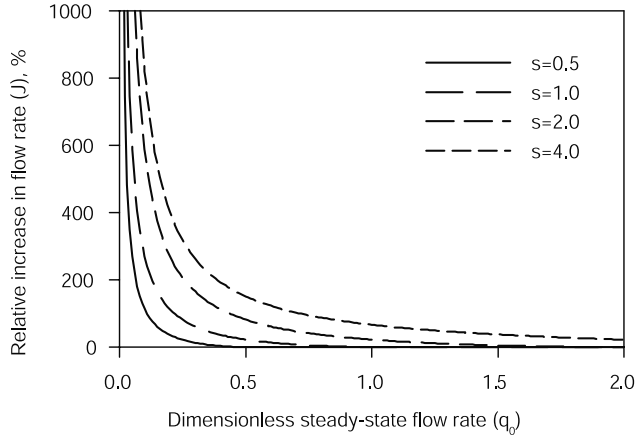

Figure 10. Relative increase in capillary flow rate due to vibrations versus steady state flow rate (no vibrations applied) for various values of the effective amplitude of vibration s.

and taking half of the value calculated from equation (44), we obtain $(p_c)_{\text{crit}} \approx 400$ Pa. The value of the critical pressure gradient C will vary depending on the size of the blob L. Assuming a "bundle of capillary tubes" model [*Dullien*, 1992] and $L = 1$ m, we obtain $C = 800$ Pa/m, which is within the range of the critical pressure gradients estimated for a yield stress fluid (see section 2.6). Similarly, for $L = 0.1$ m, the critical pressure gradient will be $C = 8000$ Pa/m. This demonstrates that, within our model, the oil at very low residual saturation [*Dullien*, 1992; *Nikolaevskiy et al.*, 1996] will be difficult to mobilize even at high intensities of acoustic stimulation.

[47] To further analyze the effects of vibration on capillary trapping and emphasize its analogy with the yield stress behavior, we again use the dimensionless variables (equation (22)), with the critical pressure gradient G_{crit} (equation (14)) replaced by C (equation (43)). Figure 8 presents the average percolation rate of the blob q, calculated from equations (21), (22), and (42)–(44), as a function of external pressure gradient g. Figure 9 demonstrates the dependence of q on the amplitude s for different values of g. Figure 10 shows the relative increase in the capillary flow rate (equation (24)). All curves bear significant resemblance to the relevant plots for the yield stress model (Figures 2–4), in that vibrations decrease the critical pressure gradient at which the blob is mobilized, as well as increase its percolation rate.

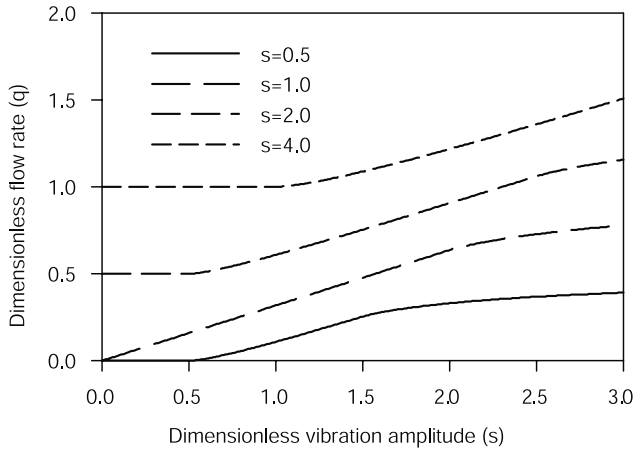

Figure 9. Dimensionless flow rate q of a capillary blob versus effective vibration amplitude s, for various values of the dimensionless pressure gradient g.

4. Conclusions

[48] In this paper, we theoretically investigated the effect of low-frequency sonic vibrations on the flow of NAPLs through a porous medium, focusing on two distinct and related physical mechanisms: the yield stress rheology of the pore-filling fluid and capillary trapping. Both mechanisms are found to produce similar behavior at the macroscopic level. As follows from empirical data, both can be important players in the mobilization of reservoir fluids in acoustic stimulation technologies.

[49] We have found that vibrations can significantly decrease the value of minimum pressure gradient required to mobilize entrapped fluid, as well as increase the average flow rate. The effects of vibrations are most pronounced in the zones of relatively low pressure gradients, and will be small if the external pressure gradient is high. The theory thus indicates that the application of sound can increase the efficiency of secondary and tertiary oil recovery methods, as suggested based on vast empirical data by the authors of a literature review [*Beresnev and Johnson*, 1994].

[50] The intensity of the sonic field required to provide practically significant effect in the mobilization of entrapped fluids is on the order of 0.2–125 W/m^2, depending on the frequency and the parameters of the porous medium and the fluids, which is achievable with the available sonic transducers [*Beresnev and Johnson*, 1994].

[51] The development of a quantitative physical theory of the effects of sound on fluid percolation in rock has been a major impediment in the applications of sonic stimulation technologies. While our theory does not serve an exhaustive description of all possible phenomena in play, it provides a model based on realistic assumptions, which can be used as guidance in emerging field applica-

tions or a starting point in the development of future, more comprehensive theories.

References

Aarts, A. C. T., and G. Ooms, Net flow of compressible viscous fluid induced by travelling waves in porous media, *J. Eng. Math.*, *43*, 435–450, 1998.

Bear, J., *Dynamics of Fluids in Porous Media*, Dover, Mineola, N.Y., 1988.

Beresnev, I. A., and P. A. Johnson, Elastic-wave stimulation of oil production: A review of methods and results, *Geophysics*, *59*(6), 1000–1017, 1994.

Biot, M. A., Theory of propagation of elastic waves in a fluid-saturated porous solid, I, Low-frequency range, *J. Acoust. Soc. Am.*, *28*, 168–178, 1956.

Bird, R. B., R. C. Armstrong, and O. Hassager, *Dynamics of Polymeric Liquids*, vol. 2, 2nd ed., John Wiley, New York, 1987.

Chang, C., Q. D. Nguyen, and H. P. Rønningsen, Isothermal startup of pipeline transporting waxy crude oil, *J. Non Newtonian Fluid Mech.*, *87*, 127–154, 1999.

Charlaix, E., and H. Gayvallet, Dynamics of a harmonically driven fluid interface in a capillary, *J. Phys. II*, *2*, 2025–2038, 1992.

de Gennes, P. G., Wetting: Statics and dynamics, *Rev. Mod. Phys.*, *57*(3), 827–863, 1985.

del Rio, J. A., M. L. de Haro, and S. Whitaker, Enhancement in the dynamic response of a viscoelastic fluid flowing in a tube, *Phys. Rev. E*, *58*(5), 6323–6327, 1998.

Drake, T., and I. Beresnev, Acoustic tool enhances oil production, *Am. Oil Gas Rep.*, 101–105, Sept. 1999.

Dullien, F. A. L., *Porous Media: Fluid Transport and Pore Structure*, Academic, San Diego, Calif., 1992.

Goshawk, J. A., and N. D. Waters, The effect of oscillation on the drainage of an elastico-viscous liquid, *J. Non Newtonian Fluid Mech.*, *54*, 44–464, 1994.

Hilpert, M., G. H. Jirka, and E. J. Plate, Capillary-induced resonance of oil blobs in capillary tubes and porous media, *Geophysics*, *65*(3), 874–883, 2000.

Kazakia, J. Y., and R. S. Rivlin, The influence of vibration on Poiseuille flow of a non-Newtonian fluid, I, *Rheol. Acta*, *17*(3), 210–226, 1978.

Leger, L., and J. F. Joanny, Liquid spreading, *Rep. Prog. Phys.*, *55*, 431–486, 1992.

Mena, B., O. Manero, and D. M. Binding, Complex flow of viscoelastic fluids through oscillating pipes: Interesting effects and applications, *J. Non Newtonian Fluid Mech.*, *5*, 427–448, 1979.

Nikolaevskiy, V. N., *Geomechanics and Fluid Dynamics with Applications to Reservoir Engineering*, Kluwer Acad., Norwell, Mass., 1996.

Nikolaevskiy, V. N., G. P. Lopukhov, Y. Liao, and M. J. Economides, Residual oil reservoir recovery with seismic vibrations, *SPE Prod. Facil.*, SPE29155, 89–94, May 1996.

Pan, Y., and R. N. Horne, Resonant behavior of saturated porous media, *J. Geophys. Res.*, *105*(B5), 11,021–11,028, 2000.

Papanastasiou, T. C., Flow of materials with yield, *J. Rheol.*, *31*(5), 385–404, 1987.

Rahaman, K. D., and H. Ramkissoon, Unsteady axial viscoelastic pipe flow, *J. Non Newtonian Fluid Mech.*, *57*, 27–38, 1995.

Roberts, P. M., A. Sharma, V. Uddameri, M. Monagle, D. E. Dale, and L. K. Steck, Enhanced DNAPL transport in a sand core during dynamic stress stimulation, *Environ. Eng. Sci.*, *18*(2), 67–79, 2001.

Schetz, J. A., and A. E. Fuhs, *Fundamentals of Fluid Dynamics*, John Wiley, New York, 1999.

Spanos, T. J. T., M. B. Dusseault, and B. Davidson, Pressure pulsing at the reservoir scale as new EOR approach, *Proc. CSPG Pet. Soc. Pap.*, *99-11*, Can. Soc. of Pet. Geol., Calgary, Alberta, 14–18 June 1999.

Telford, W. M., L. B. Geldart, and R. E. Sheriff, *Applied Geophysics*, 2nd ed., Cambridge Univ, Press, New York, 1996.

Tsiklauri, D., and I. Beresnev, Enhancement in the dynamic response of a viscoelastic fluid flowing through a longitudinally vibrating tube, *Phys. Rev. E*, *63*, 046304-1–046304-4, 2001a.

Tsiklauri, D., and I. Beresnev, Non-Newtonian effects in the peristaltic flow of a Maxwell fluid, *Phys. Rev. E*, *64*, 036303-1–036303-5, 2001b.

Wang, H. F., *Theory of Linear Poroelasticity With Applications to Geomechanics and Hydrogeology*, Princeton Univ. Press, Princeton, N.J., 2000.

Wardhaugh, L. T., and D. V. Boger, The measurement and description of the yielding behavior of waxy crude oils, *J. of Rheol.*, *35*(6), 1121–1156, 1991.

I. A. Beresnev and P. P. Iassonov, Department of Geological and Atmospheric Sciences, Iowa State University, 253 Science I, Ames, Iowa, 50011-3212, USA. (iassonov@iastate.edu)